Proceedings of the World Congress on Mechanical, Chemical, and Material Engineering (MCM 2015)
Barcelona, Spain – July 20 - 21, 2015
Paper No. 290

Impacts of Electroosmosis Forces on Surface-Tension-Driven Micro-Pumps

Khodayar Javadi, Hamid Moezzi-Rafie
Sharif University of Technology, Department of Aerospace Engineering
Azadi Street, Tehran, Iran
kjavadi@sharif.ir; moezzi@ae.sharif.edu

Vahid Goodarzi-Ardakani
Sharif University of Technology, Department of Aerospace Engineering
Azadi Street, Tehran, Iran
goodarzi_vahid@ae.sharif.edu

Abstract **-**The purpose of this work is to investigate the influences of the electro-osmosis forces on the performance of a surface tension driven passive micro-pump. This work is in continuation of our previous work in which a surface tension driven passive micro-pump was numerically simulated for the first time. In this work, electroosmosis forces are inserted on the side walls of a 2D micro-channel. A water droplet, which is equivalent to a circle of radius ~1.07 mm in 2D domain, is placed onto an entry port of 1.8 mm diameter. The contact angle of the inlet droplet is considered 122.74 degrees. The entry port is connected to the exit port via a 5 mm long rectangular micro-channel. The height of the micro-channel and the entry and exit ports are 0.1 and 1.1 mm respectively. Another water droplet is placed onto the exit port of 2.5 mm diameter and the droplet diameter is considered such that its maximum height from the port is 0.4 mm. The electroosmosis forces are changed from $1e^5$ to $1e^6$.

Keywords**:** Passive Micro-pump, Surface Tension Driven Flow, Electroosmotic Flow, Micro-fluidics, MEMS.

1. Introduction

One of the most challenging tasks in developing a fully integrated micro-fluidic system has been the development of efficient and reliable micro-pumps (Laser and Santiago (2004), Au et al. (2011), Nguyen et al. (2002), Abhari et al. (2012)). In macro-scale, a number of pumping techniques exist such as peristaltic pumps, vacuum-driven pumps, venturi-effect pumps, etc. However, in micro-scale, most mechanical pumps rely on pressurizing the working fluid and forcing it to flow through the system (Bhushan (2010)). A passive system is defined inherently as one that does not require an external energy. In the simplest case, a small droplet of a fluid is placed at one end of a straight micro-channel, and a much larger droplet of the fluid is placed at the opposite end of the micro-channel. The pressure within the small droplet is significantly higher than the pressure within the large droplet, due to the difference in the surface tension effects across the two droplets. Consequently, the liquid will flow from the small droplet and add to the larger droplet. The flow rate can be varied by changing various parameters such as the volume of the pumping droplet, the surface free energy of the liquid, or the resistance of the micro-channel, etc. This pumping scheme is very easy to realize and can be used for a wide variety of fluids. Walker and Beebe (2002), have demonstrated pumping action using the difference between the surface tension pressure at the inlet and outlet of a micro-fluidic channel. Berthier and Beebe (2007), presented an analytical solution and a two phase model to describe the flow in passive pump driven micro-fluidic devices. Also Chen et al. (2008), in order to provide a generally applicable description of the passive pump surface tension driven flow in micro-channels, reported on numerical modelling of volume flow rate as function of time for different experimental conditions.

Computer simulations can help understand the basic fluid physics, as well as enable design of experiments or systems for use in micro-fluidics. Yang et al. (2001), using a finite difference approach analysed numerically the electroosmotic flow in micro-channels. Chai and Shi (2007) introduced a new lattice Boltzmann model for simulation of electroosmotic flow in micro-channels.

In this paper, passive pumping was analysed and presented numerically using a computational fluid dynamics (CFD) finite element based approach in a 2D domain. Also, with the aid of applying an electric field, we have studied the effect of electroosmotic velocity on the pumping performance. Based on our literature review, there is no numerical studies on this issue before this work.

2. Problem Formulation

The equations govern the problem are N-S for two phase flow:

$$\rho \frac{\partial u}{\partial t} = F_{st} + \nabla.\left[-pI + \mu\left(\nabla u + (\nabla u)^T\right] + \rho g + F \right. \quad (1)$$

$$\nabla. u = 0 \quad (2)$$

I is the identity matrix, μ is dynamic viscosity of the fluid and F is a body force which is neglected here. F_{st} is the surface tension force defined as:

$$F_{st} = \sigma(\nabla_s . \mathbf{n}_i)\mathbf{n}_i - \nabla_s \sigma \quad (3)$$

where ∇_s is the surface gradient operator $\nabla_s = (I - \mathbf{n}_i \mathbf{n}_i^T)\nabla$ and σ is the surface tension at the interface.

At the walls of inlet and outlet ports and the rectangular micro-channel, no-slip boundary condition is used.

In the case of considering the electroosmosis impacts on the passive micro pumping, since the thickness of the electric double layer is typically on the order of nano-meters, one can define the electroosmotic flow velocity, u_{eof} , as the velocity boundary condition:

$$u_{eof} = \mu_{eof} E \quad (4)$$

Where E is the strength of the electric field applied tangential to the surface and μ_{eof} is the electroosmotic mobility defined as:

$$\mu_{eof} = \frac{\varepsilon_r \varepsilon_0 \zeta}{\mu} \quad (5)$$

Where ε_r is the relative permittivity of material between two electrodes, ε_0 = $8.8541878176 \times 10^{-12}$ F/m, is the vacuum permittivity and ζ is the zeta potential. The zeta potential, an experimentally observed quantity, is the electrokinetic potential at the edge of the Stern layer[1].

3. Results and Discussion

Prior to go through results discussion section the numerical simulation is verified in the following section.

[1] Ions in the liquid are strongly drawn toward the surface and form a very thin layer called the Stern layer in which the ions in the liquid are paired with the charges on the surface.

3. 1. Validation with Previous Experimental Data

In order to describe the flow motion in the micro-channel, a 2D model was developed. A 2D water droplet, which is equivalent to a circle of radius ~1.07 mm, is placed onto an entry port of 1.8 mm diameter. The contact angle of the inlet droplet is considered to be about 122.74 degrees. The entry port is connected to the exit port via a 5 mm long rectangular micro-channel. The height of the micro-channel and the entry and exit ports are 0.1 and 1.1 mm respectively. Another water droplet is placed onto the exit port of 2.5 mm diameter and the droplet diameter is considered such that its maximum height from the port is 0.4 mm (Fig. 1). The geometry and properties of the device and the droplets are approximately (not exactly) similar to Chen et al. (2008) model and the results are validated with their work.

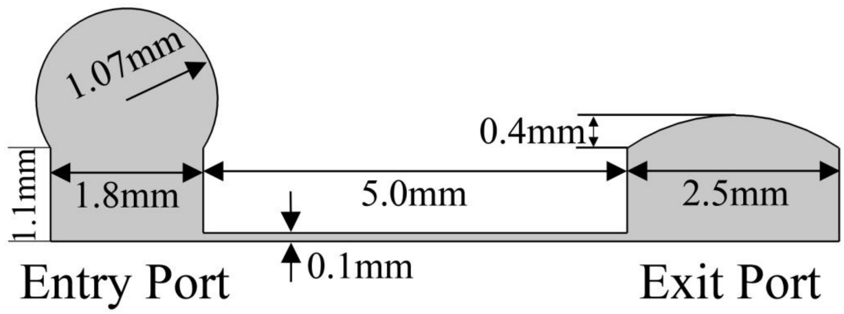

Fig. 1. Geometry of the present model.

The flow was simulated for 60 seconds and the average velocity at the middle of micro-channel obtained for 30 seconds. Present results with about 31038 mesh elements and the experimental and analytical solution (using Young-Laplace equation) of the work of Chen et al. (2008), are shown in Fig. 2. Also a typical velocity magnitude contour at 1.5 seconds after the pumping initiation is shown in Fig. 3. According to Fig. 2, the discharge velocity of the fluid from the 2D sample droplet reaches zero at approximately 12 seconds while, the discharge velocity of the fluid from the spherical sample droplet of the analytical and experimental work of Chen et al. (2008), becomes zero at about 22 seconds and a bit later respectively. The time difference between the simulation and the analytical solution and also the experiment is due to geometrical differences between one another. Also, according to Young-Laplace equation, the pressure at the interface of a droplet is defined as:

$$\Delta P = \gamma \left(\frac{1}{R_1} + \frac{1}{R_2}\right) \tag{6}$$

In the case of a spherical droplet i.e. 3D domain, $R_1 = R_2$; so the pressure at the interface becomes $2\gamma/R$. But in the case of a 2D droplet, one of the radii goes to infinity; so the pressure at the interface becomes γ/R. The smaller pressure difference results in smaller velocity magnitude. Also, in comparison with the analytical solution (Young-Laplace equation) of Chen et al. (2008) and also their experiment, the velocity in the micro-channel for the 2D droplet reaches zero sooner. Although our model works well, the differences in obtaining of the droplets radii and contact angles between our model and the selected experiment have caused such inequalities.

3. 2. Grid Study

Grid dependency was checked for three different grid sizes including 20045, 31038 and 54800 mesh elements. The grid structure at the middle of micro-channel for these grid sizes is shown in Fig. 4.

Due to very small dimension and also the Stokes flow regime, if the mesh in the micro-channel is not fine enough, then we would have a false zero velocity magnitude. Therefore, meshing is one of the most vital issues in this simulation. The average velocity magnitude at the middle of micro-channel for those different grid sizes mentioned above, is shown in Fig. 5. As it can be seen, there is no significant difference between the velocity curve for meshes with 31038 and 54800 elements. The difference seen between the mesh with 20045 with meshes with 31038 and 54800 elements is due to the fact that we have lower elements across the micro-channel. In the present model, to consume less time and CPU, a mesh of containing 31038 elements was used. It is necessary to mention that the grid size in the micro-channel is much more important than the one in the ports and droplets.

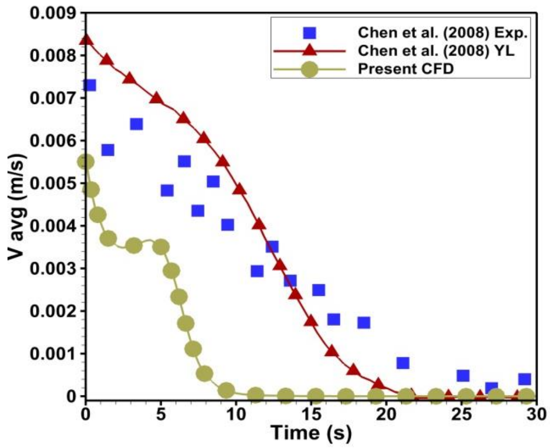

Fig. 2. Comparison of the discharge velocity of fluid from our 2D sample droplet and work of Chen et al. (2008).

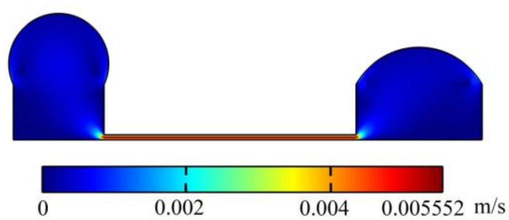

Fig. 3. Velocity magnitude contour at 1.5 seconds after the pumping initiation.

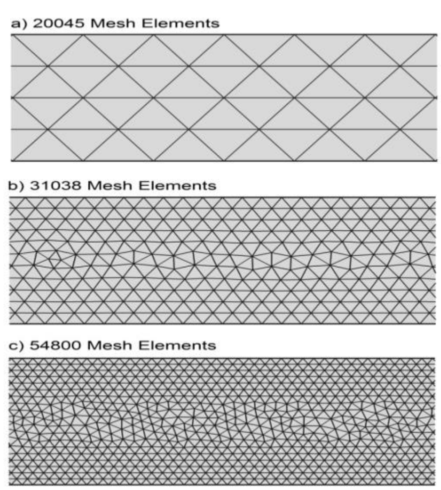

Fig. 4. Different numbers of mesh elements in the micro-channel region. (a) 20045 elements. (b) 31038 elements. (c) 54800 elements.

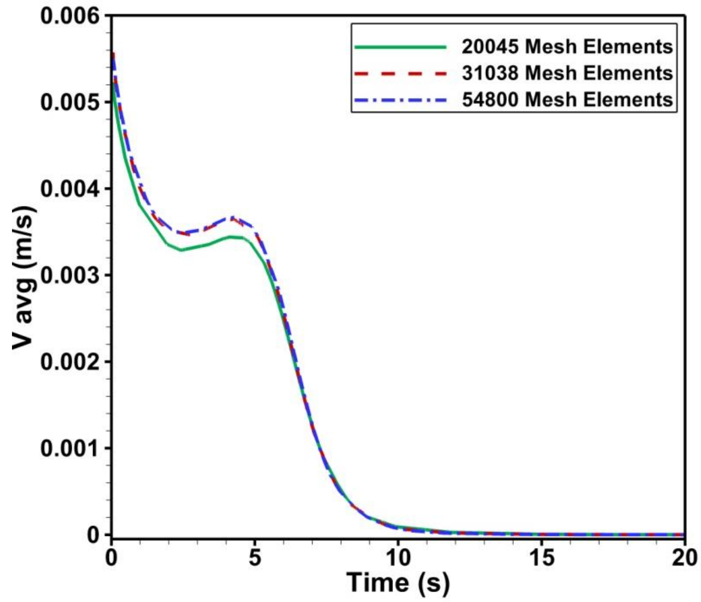

Fig. 5. Grid study for different numbers of elements.

3. 4. The Effect of Electroosmotic Velocity on the Pumping Performance

When a polar liquid (for example water) and a solid come into contact, the solid surface acquires an electric charge, which influences the charge distribution within the liquid and the electric double layer or EDL will be generated. The charges close to the wall are strongly drawn toward the surface, but the application of an electric field can change the charge distribution deeper in the fluid. Here, we apply an electric field to the micro-channel and since the EDL thickness is of the order of nano-meters, we can consider the electroosmotic flow velocity u_{eof} as the boundary velocity (refer to equ. (4)) instead of for example no slip boundary condition. The strength of the electric field varies between 10^5 to 10^6 V/m. Relative permittivity and zeta potential are considered 80 and -2 mV respectively.

Fig. 6, Compares the velocity profiles at different locations 10 and 15 seconds after the pumping initiation for three different applied electric fields of zero (no slip condition), 10^5 to 10^6 V/m . From the figure, it is clear that the more the applied electric field, the more fluid acceleration adjacent to the wall. Also, it is obvious from the figure that the velocity distribution inside the micro-channel is asymmetric. The reason is that the flow is under the influence of inlet and outlet effects of the channel. Another consequence of these figures is that applying electric field on the micro-channel can be a powerful tool for flow control in these problems.

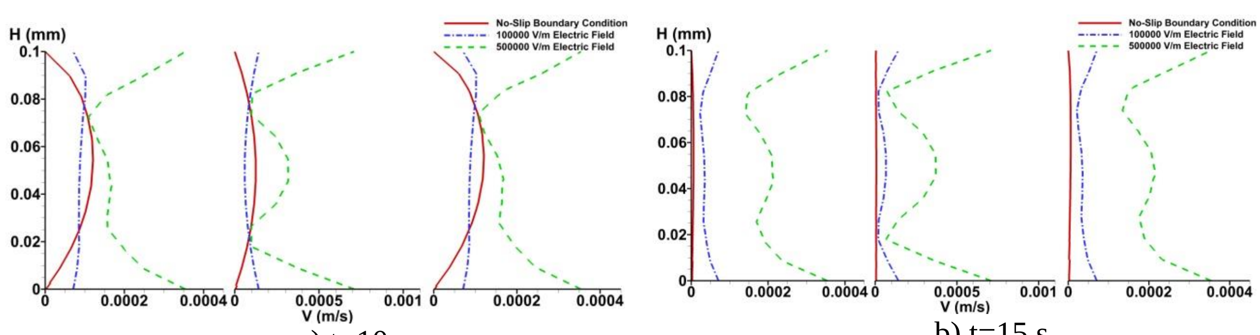

Fig. 6. Velocity profiles at 10 seconds after the pumping initiation at the inlet and outlet of a micro-channel with 5 mm length and 0.1 mm height.

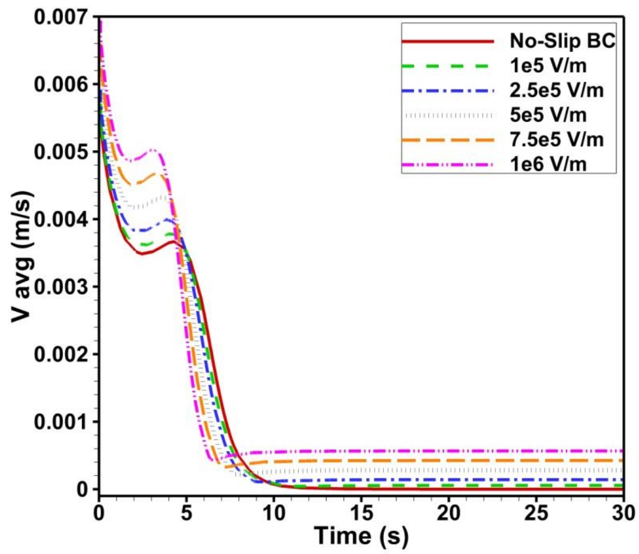

Fig. 7. Comparison of average velocity magnitude at the middle of micro-channel for no slip boundary condition and electroosmotic velocity boundary condition with different electric field strengths.

The average velocity magnitude at the middle of micro-channel in the case of coupling this effect with the passive pumping is shown in Fig. 7 Of course, notice that when applying the electric field, the passive micro-pump somehow changes to passive-active ones (i.e. an external driving force has been applied). According to Fig. 7, as the electric field strength increases, the initial discharge velocity of fluid from the sample droplet increases and also the time when the velocity in the micro-channel reaches a constant value decreases.

4. Conclusion

The paper numerically investigates a passive surface tension driven micro-pump with the presence of exerted electro-osmosis forces on the sides of the micro-channel. The amount of exerted forces varies between $1e^5$ to $1e^6$ V/m. Results shows that applied electro-osmosis forces causes an axial accelerating on the operating flow. The more increase in the exerted electro-osmosis force, the more acceleration of the operating fluid. The results also clarify that applying electrical field at the boundaries is a useful and powerful tool for flow control purposes.

References

Abhari, F., Jaafar, A., & Md Yunus, N. A. (2012). A Comprehensive Study of Micropumps Technologies. *International Journal Of Electromechanical Science,* 7, 9765-9780.

Au, A. K., Lai, H., Utela, B. R., & Folch, A. (2011). Microvalves and Micropumps for BioMEMS. *Micromachines,* 2, 179-220.

Berthier, E., & Beebe, J. D. (2007). Flow Rate Analysis of a Surface Tension Driven Passive Micropump. *Lab Chip,* 7, 1475–1478.

Bhushan, B. (2010). Springer Handbook of Nanotechnology 3rd edition.

Chai, Z., & Shi, B. (2007). Simulation of Electroosmotic Flow in Microchannel with Lattice Boltzmann Method. *Physics Letters A*, 364, 183–188.

Chen, I. J., Eckstein, C. E., & Lindner, E. (2008) Computation of Transient Flow Rates in Passive Pumping Micro-fluidic Systems. *Lab Chip,* 9, 107–114.

Laser, D. J., & Santiago, J. G. (2004). A Review of Micropumps. *Journal of Micromechanics and Microengineering,* 14, R35–R64.

Nguyen, N-T, Huang, X., & Chuan, T. K. (2002). MEMS-Micropumps: A Review. *Journal of Fluids Engineering*, 124.

Walker, G. M., Beebe, D. J. (2002). A Passive Pumping Method for Microfluidic Devices. *Lab Chip*, 2, 131–134.

Yang, R.-J., Fu, L.-M., & Lin, Y.-C (2001). Electroosmotic Flow in Microchannels. *Journal of Colloid and Interface Science*, 239, 98–105.